

# Jets in GRBs: Tests and Predictions for the Structured Jet Model

Rosalba Perna<sup>1,2,3</sup>, Re'em Sari<sup>3</sup> and Dale Frail<sup>4</sup>

## ABSTRACT

The two leading interpretations of achromatic breaks that are observed in the light curves of GRBs afterglow are (i) the manifestation of the edge of a jet, which has a roughly uniform energy profile and a sharp edge and (ii) a line of sight effect in jets with a variable energy profile. The first scenario requires the inner engine to produce a jet with a different opening angle each explosion, while the latter requires a standard engine. The physical structure of the jet is a crucial factor in understanding GRB progenitors, and therefore discriminating the two jet scenarios is particularly relevant. In the structured jet case, specific predictions can be made for the distribution of observed break angles  $\theta_{\text{break}}$ , while that distribution is arbitrary in the first scenario. We derive the theoretical distribution for the structured jet model. Specifically, we predict the most common angle to be about 0.12 rad, in rough agreement with the sample. If this agreement would hold as the sample size increases, it would strengthen the case for the standard jet hypothesis. We show that a prediction of this model is that the average viewing angle is an increasing function of the survey sensitivity, and in particular that a mission like *Swift* will find the typical viewing angle to be about 0.3 rad. The local event rate predicted by this model is  $R_{\text{GRB}}(z = 0) \sim 0.5 \text{ Gpc}^{-3} \text{ yr}^{-1}$ .

*Subject headings:* gamma rays: bursts — cosmology: theory

## 1. Introduction

The degree to which gamma-ray bursts (GRBs) and their afterglows are beamed is an important issue. A proper understanding of the geometry of the relativistic outflow affects the total energetics of GRB central engines and the GRB event rates, both of which are crucial parameters for constraining possible progenitor models. Evidence for non-isotropic outflows is believed to come from observations of achromatic breaks in afterglow light curves (e.g., Rhoads 1999, Sari et al. 1999) and the detection of polarized emission (Covino et al. 1999, Wijers et al. 1999). We should

---

<sup>1</sup>Harvard Society of Fellows, 74 Mount Auburn Street, Cambridge, MA 02138

<sup>2</sup>Harvard-Smithsonian Center for Astrophysics, 60 Garden Street, Cambridge, MA 02138

<sup>3</sup>130-33, California Institute of Technology, Pasadena, CA 91125

<sup>4</sup>National Radio Astronomy Observatory, P.O. Box O, Socorro, NM, 87801

however note that, whereas this is a natural interpretation for the breaks, in some cases other interpretations have been proposed or different conclusions derived (e.g. Nicastro et al. 1999; Vrba et al. 2000). Here we adopt the point of view that the observed breaks are indeed manifestations of jets.

In early theoretical papers (e.g., Rhoads 1997, Sari et al. 1999) it was assumed for simplicity that the ejecta had to be distributed approximately uniform across the entire opening angle in the gamma-ray phase and that the majority of the explosive energy in the afterglow phase must have a single bulk Lorentz factor. In this “uniform” model, a break occurring in the light curves at  $t_{\text{break}}$  can be directly translated into a jet with an opening angle  $\theta_{\text{break}}$ . Using this simple framework, Frail et al. (2001) carried out an analysis of all known afterglows and found that there was a distribution of jet opening angles leading to a reduction in the gamma-ray energy from its isotropic value with relatively small scatter. The observed distribution was shown to be heavily weighted towards small opening angles.

Rather than positing a uniform jet, it is equally reasonable to assume that GRB jets are structured in some fashion. In the collapsar progenitor model (e.g. Wang, Woosley & MacFadyen 2002) the Lorentz factor and energy are high near the rotation axis, but decrease off axis as the degree of entrainment increases. Salmonson (2000) has argued for such a jet structure to explain the empirical correlation between the GRB peak luminosity and pulse lag (Norris et al. 2000). In this case, the distribution of observed break times in afterglow light curves are not due to a distribution of opening angles but rather originate from variations in the viewing angle of a structured jet (Postnov, Prokhorov & Lipunov 2001). In two recent papers by Rossi, Lazzati & Rees (2002a) and Zhang & Meszaros (2002) it was shown that a jet with a universal beaming configuration could reproduce the near-constant energy result of Frail et al. (2001) provided that the energy per unit solid angle (and Lorentz factor) varied as the inverse square of angular distance from the jet symmetry axis.

Discriminating between the uniform and structured jet models is important as they yield different estimates for the true GRB event rate and the total energy, besides leading to clues on the physical mechanism producing the jet itself. Afterglow lightcurves have argued to be degenerate to the structure of the jet (Rossi et al. 2002a, Zhang & Meszaros 2002) and therefore they cannot be used as diagnostics. Rossi et al. (2002b) showed that detection of polarization can provide useful constraints. Here we concentrate on diagnostics based on geometrical effects. In particular, in the structured jet model, since the inferred opening angle is just a geometric effect of the viewing angle, it is possible to predict the distribution of angles and compare it to the *observed* distribution of  $\theta_{\text{break}}$  by Frail et al. (2001) and Bloom et al. (2003). Unfortunately, a specific prediction is not possible for the uniform model, since there is no framework for jet formation which yields the distribution of opening angles.

In this paper, we work out the expected distribution of burst opening angles, under the structured jet scenario and given various assumption of the star formation rate evolution in the universe.

We find two competing effects. First, even though randomly oriented bursts would be rarely observed on axis, they are much brighter and therefore can be seen to larger distances rendering small opening angles common. Cosmological effects limit the volume at large redshifts leading to an effective cutoff at the small opening angle. As a result, we predict that the most common opening angle should be about 0.12 rad. Furthermore, under the structured jet model, we predict that more sensitive future missions like SWIFT, will find a much larger typical angle, about 0.3 rad.

The observed data so far is still a small sample. Selection effects are hard to quantify, especially for large and small opening angles. In addition, the variety of instruments with different sensitivity used to detect the bursts, makes a robust conclusion difficult at this stage. Yet, we show that the current set of data, as given in the most updated sample of Bloom et al. (2003), is at least in rough agreement with the distribution we predict for the structured jet model. If this conclusion would hold with much larger and less biased sample, it would be a strong support to the structured jet model.

## 2. Computation of the observed distribution of jet angles

### 2.1. Scalings for a Euclidian universe

If all bursts were observable, then we would expect that the number  $dn(\theta)/d\theta$  of bursts with angle in the interval  $d\theta$  around  $\theta$  would be proportional to  $\theta$ . This implies that most of the observed bursts should have a large angle, which is in complete contradiction with observations. Zhang & Meszaros (2002) attributed this apparent discrepancy to the small sample size or afterglow selection effects. However, this argument does not account for the fact that bursts with small  $\theta$  are brighter by a factor of  $\theta^{-2}$ , and therefore can be seen (in an Euclidian universe) up to a distance  $\theta^{-1}$  farther, which contains a volume larger by a factor of  $\theta^{-3}$ . The expected distribution in Euclidean geometry is therefore expected to be  $dn/d\theta \propto \theta^{-2}$ . Although this is closer to what observations suggest, we will show that this now exaggerates the number of small-angle bursts compared to a proper cosmological prediction: GRBs originate at redshifts of order unity, and therefore suffer considerable cosmological corrections. This is why their  $\log N - \log S$  curve does not obey the Euclidian  $S^{-3/2}$ , but is shallower at low  $S$ . It is for the same reason that the number of observed bursts of low  $\theta$  will not be as high as predicted by the Euclidian  $\theta^{-2}$ . In the following, we work out these cosmological effects in detail.

## 2.2. Cosmological effects

Let  $R_{\text{GRB}}(z)$  be the GRB rate per unit comoving volume per unit time, then the total (i.e. over the all sky) rate of bursts with inferred jet angle between  $\theta$  and  $\theta + d\theta$  is given by

$$\frac{dn(\theta)}{d\theta} = \sin \theta \int_0^{z_{\text{max}}(\theta)} dz \frac{R_{\text{GRB}}(z)}{(1+z)} \frac{dV(z)}{dz}, \quad (1)$$

where  $z_{\text{max}}(\theta)$ , is the maximal redshift up to which we can observe a burst with apparent angle  $\theta$ . This redshift is found by numerically inverting the equation

$$F_{ph,\text{lim}} = \frac{L_{ph}(\theta)}{4\pi D^2 (z_{\text{max}})(1+z_{\text{max}})^\alpha}, \quad (2)$$

where  $F_{ph,\text{lim}}$  is the limiting photons flux (photons per unit area per unit time) that is detectable by the GRB detector with frequency range,  $\nu_l < \nu < \nu_u$ .  $L_{ph}(\theta)$  is the photons luminosity (photons per unit time) in the same frequency range but in the local frame of the burst, of a burst with an apparent angle  $\theta$ . A factor of  $(1+z)^{\alpha-1}$  is a spectral correction, assuming that the GRB has a differential photon spectral index  $\alpha$ , and another factor of  $1+z$  takes care of time dilation. For BATSE,  $\nu_l = 50$  keV and  $\nu_u = 300$  keV.

The normalization constant is determined by the condition

$$\frac{L_{\nu_1-\nu_2}}{4\pi} 2\pi\theta^2 T = E \quad (3)$$

where  $E \approx 10^{51}$  ergs is the roughly constant energy of GRBs as inferred by (Bloom et al. 2003). That relation used the luminosity integrated over the frequency range  $\nu_1 = 20$  keV to  $\nu_2 = 2000$  keV as calculated by Bloom et al. (2001). For powerlaw photon spectrum, this is related to the photon luminosity in the triggering band  $\nu_l \nu_h$  by

$$L_{ph}(\theta) = \frac{2E}{\theta^2 T h \nu_l} \frac{\alpha - 2}{\alpha - 1} \left(\frac{\nu_l}{\nu_1}\right)^{-\alpha+2} \frac{1 - (\nu_u/\nu_l)^{-\alpha+1}}{1 - (\nu_2/\nu_1)^{-\alpha+2}} \quad (4)$$

If we take a spectrum with  $\alpha \approx 1$ , (which is appropriate for the frequency range 50 – 300 keV as reported by Mallozzi et al. 1996) then we obtain,

$$L_P(\theta) = 1.1 \times 10^{57} T^{-1} \theta^{-2} \text{ ph sec}^{-1}. \quad (5)$$

It should be noted that  $T$  is not the total duration of the burst, but an “effective” duration of convenience here, that is the duration that the burst would have if its energy output were constant at the peak value rather than highly variable. In the simplest version of our model (§2 & 3), we will assume a single value of  $T$  for all the bursts; however we will explore (§4) how our results vary when a scatter in  $T$  is introduced (which is a more realistic assumption).

The jet model with the energy profile  $\propto \theta^{-2}$  also makes detailed predictions for the observed GRB flux distribution. This, within our formalism, can be written as

$$\frac{dn(S)}{dS} = \int_0^\infty dL_p f(L_p) \left[ \frac{R_{\text{GRB}}(z)}{(1+z)} \frac{dV(z)}{dz} \left| \frac{dz}{dS}(z, L_p) \right| \right]_{z=z(S, L_p)} \quad (6)$$

where, given Eq. (5), the luminosity function takes the form  $f(L_p) \propto L_p^{-2}$ .

In Eqs.(1) and (6),  $dV(z)/dz$  is the comoving volume. In a flat cosmology with a cosmological constant it is given by

$$\frac{dV(z)}{dz} = 4\pi D^2(z) \frac{dD(z)}{dz} \quad (7)$$

where  $D(z)$  is the comoving distance,

$$D(z) = \frac{c}{H_0} \int_0^z \frac{dz'}{\sqrt{(1 + \Omega_m z)(1 + z')^2 - \Omega_\Lambda (2z' + z'^2)}} \quad (8)$$

We assume a cosmological model with  $\Omega_m = 0.3$ ,  $\Omega_\Lambda = 0.7$  and  $H_0 = 71 \text{ km s}^{-1} \text{ Mpc}^{-1}$ .

We assume that GRBs trace the star formation history and we adopt, as our “standard” model for  $z \lesssim 10$ , the Rowan-Robinson star formation rate which can be fitted with the expression

$$R_{\text{GRB}}(z) = \begin{cases} R_0 10^{0.75z}, & z < z_{\text{peak}} \\ R_0 10^{0.75z_{\text{peak}}}, & z \geq z_{\text{peak}} \end{cases} \quad (9)$$

where  $z_{\text{peak}} \sim 2$ . For  $z \gtrsim 10$ , in our standard model we use an interpolation that follows the star formation history derived in numerical simulations by Gnedin & Ostriker (1997). While using this SFR as our working model, we also explore the effects on the predicted distribution  $dn/d\theta$  of different star formation histories, and in particular we consider two opposite extremes, one in which the SFR does not rapidly decline for  $z \gtrsim 10$  as implied in the numerical simulations of Gnedin & Ostriker, and another, the Madau curve (Madau 1996), in which the SFR rapidly declines at redshifts  $z \gtrsim 3$ .

For each model for the SFR, the normalization constant  $R_0$  is determined by the condition

$$\int_0^{\pi/2} d\theta \frac{dn(\theta)}{d\theta} = R_{\text{GRB}}^{\text{obs}} \quad (10)$$

where  $R_{\text{GRB}}^{\text{obs}} = 667 \text{ yr}^{-1}$  is the observed BATSE rate, and  $F_{\text{lim}}$  in Eq. (2) is the BATSE threshold flux for which this rate has been measured. We adopted the 90% efficiency peak flux threshold for BATSE, that is  $F_{\text{lim}} = 0.424 \text{ ph/sec}$  (e.g. Mallozzi, Pendleton & Paciesas 1996).

### 3. Comparison with data and predictions for more sensitive surveys

In order to compare the theoretical distributions derived in §2.2, we require a sample of gamma-ray bursts whose values of  $\theta_{\text{break}}$  have been measured. The largest published sample of  $\theta_{\text{break}}$  values

at the time of our work comes from the analysis of 28 bursts with redshifts and well-studied afterglow light curves by Bloom et al. (2003). This list of 28 includes *all* bursts with measured redshifts at this time. For all but four, some limit on  $\theta_{\text{break}}$  was derived. The exceptions are GRB 970228, in which sparse data together with likely contribution from a supernovae makes it difficult to interpret the lightcurve, GRB 990506 where no sufficient data exists, GRBs 980425 which had no optical counterpart, and GRB 021211 which is being analyzed at the time of writing. For eight of the remaining 24, upper or lower limits were put on the opening angle. We have not used these limits in our comparison. One could think that this would tend to have the effect of narrowing our sample distribution. However, the upper and lower limits do not tend to be at the edge of the distribution of the measured opening angles (see Table 2 of Bloom et al. 2003). They therefore do not necessarily reflect extreme cases, but cases with lower quality data. However, it should be noted that in three cases (GRBs 970828, 991216, 990705) the confidence that indeed a jet has been identified is weak, since the break was observed in a single frequency only. Finally, we should remark that the inferred values of  $\theta_{\text{break}}$  have some uncertainties. These values are indeed computed using the expression given in Frail et al. (2001):  $\theta_{\text{break}} \propto t_{\text{break}}^{3/8} (1+z)^{-3/8} E_{\text{iso}}^{-1/8} \eta_{\gamma}^{1/8} n^{1/8}$ . The measured values of  $t_{\text{break}}$  have relative errors within 30%, while for the densities a value of  $n = 10 \text{ cm}^{-3}$  is assumed for the 5 (out of 16) cases for which the data quality did not allow a self-consistent determination of the density through broad-band afterglow modelling. Finally, Bloom et al. assumed a constant value ( $\eta_{\gamma} = 0.2$ ) for the efficiency of the bursts. Whereas the dependence on  $\eta_{\gamma}$  is weak, a large spread in this not-well constrained quantity would introduce a further source of error in the determination of  $\theta_{\text{break}}$ . The combination of these caveats prevents a solid comparison of the data with our predictions, and the following comparison should be taken as a general guide for this type of analysis, while showing that the observed distribution so far does not seem to be in contradiction with the prediction of the structured jet hypothesis.

We performed a Kolmogorov-Smirnov (KS) test to assess the compatibility of the theoretical distributions with the data, and we found (see Figure 1), for the Rowan-Robinson SFR, a probability of  $\sim 90\%$  that the data are drawn from the theoretical distribution. In order to have a reasonable agreement with the data, a value  $T \sim 8$  sec is needed in the theoretical model.

As shown in Figure 1, there is little difference in the results (and in the required value of  $T$  to fit the data) between the case where the SFR drops rapidly after  $z \gtrsim 10$  (model 1), and where it keeps constant also at higher redshifts (model 2). The similarity between the distributions in model 1 and model 2 is a consequence of the combined effect of the decrease in volume at those high redshifts and the increased time dilution of the observed rate. On the other hand, for the same value of  $T$  (or equivalently peak luminosity), the distribution that uses the Madau SFR (model 3) predicts significantly more events with large angles. This is because this star formation rate drops abruptly at a redshift  $z \gtrsim 3 - 4$ , and therefore there is no much gain in the number of small- $\theta$  (i.e. brighter) events which can be seen at higher redshifts. A KS test showed that the model 3 distribution is consistent with the data (at the 40% level) if a value  $T \sim 25$  is used. A lower value for the peak luminosity is needed to shift the  $dn/d\theta$  distribution to lower  $\theta$ 's.

For a jet model to be self-consistent it is necessary that, if the distribution  $dn/d\theta$  has a good agreement with the data for certain model parameters, the corresponding  $dn/dS$  has to have a good agreement with the corresponding data for the same set of parameters. We found that with  $T \sim 8$  (as required in model 1) the peak fluxes are within a factor of a few for those bursts with measured  $\theta$ . More generally, when comparing the theoretical  $dn/dS$  distribution with the all BATSE catalogue we find a very good agreement for peak fluxes in the range  $1 \lesssim P \lesssim 15$  ph/cm<sup>2</sup>/s, and a departure (as an overprediction) at higher fluxes. However, it should be noted that, given the large number of bursts in the BATSE catalogue, a comparison with the  $dn/dS$  data distribution is much more sensitive to the model parameters than the  $dn/d\theta$  comparison. In a recent analysis, Lloyd et al. (2001) found that a good fit can be obtained with a luminosity function  $\propto L^{-2.2}$  (which would reduce the number of high  $P$  bursts with respect to our model) and a redshift evolution. Such a detailed analysis is beyond the scope of this paper given the lack of comparable wealth of data for the  $\theta$  distribution <sup>5</sup>. On the other hand, we should remark that, if we adopt the value  $T \sim 25$  required to fit the  $dn/d\theta$  distribution with the Madau SFR, then the luminosities that we predict are generally smaller than those measured for the bursts with known redshift. Therefore, in the following we will only use our model 1 with  $T = 8$  for further calculations. The corresponding cumulative distribution is shown with the solid line in the two panels in Figure 2 where it is compared to the binned, cumulative data. We should note that the size of the bins in the figure has been chosen so that there is an equal increment in the distribution for every new data point. This gives a better visual idea of the data distribution, but does not reflect the actual magnitude of the errors as described above.

Figure 3 shows the predicted evolution of the distribution of observed break angles with increasing sensitivity of the survey. In particular, we considered the 100% efficiency sensitivities corresponding to BATSE (solid line), HETE-2 and *Swift* (dashed line), and an intermediate sensitivity (dotted line). An interesting prediction of the luminosity distribution in Eq.(5) is that the average observed jet angle is an increasing function of the survey sensitivity. There are two counter-acting effects that determine the average observed jet angle  $\langle \theta \rangle$  of the sample as a function of the survey sensitivity. As  $F_{\text{lim}}$  decreases,  $z_{\text{max}}$  increases, bringing into the sample a fraction of bursts with larger redshifts and correspondingly smaller  $\theta$  (which are the most luminous). On the other hand, the higher sensitivity also brings into the sample a fraction of bursts with larger  $\theta$  at lower redshifts, and this latter effect dominates over the former, partly as a result of the volume-reduced and time-dilated rate of the high- $z$  bursts.

---

<sup>5</sup>It should also be noted that the value of the peak luminosity that best fits the  $dn/d\theta$  distribution depends on the adopted value of the detection efficiency, which may vary from burst to burst.

#### 4. Extensions

All the above results have been produced under the assumption of a strict correlation between the total energy of the burst and its peak flux. However, as discussed in §2, this relation has a scatter; therefore we have also investigated the extent to which our results change when a dispersion in the distribution of the values of  $T$  (i.e. in the relation 5) is introduced. If we parameterize the scatter in  $T$  with a probability distribution,  $P(T)$ , then the distribution of jet angles (1) is generalized to

$$\frac{dn(\theta)}{d\theta} = 2\pi \sin \theta \int_0^\infty dT P(T) \int_0^{z_{\max}(\theta, T)} dz \frac{R_{\text{GRB}}(z)}{(1+z)} \frac{dV(z)}{dz}. \quad (11)$$

We took the probability distribution for the scatter,  $P(T)$ , to be a log-gaussian distribution with mean equal to  $T = 8$ , and studied the dependence of the break-angle distribution  $dn/d\theta$  on the width of the distribution  $\sigma_T$ . A K-S test shows that, with a scatter  $\sigma_T = 0.3$ , the theoretical distribution is still compatible with the data at the 80%, while with  $\sigma_T = 0.5$  the agreement is at the 40% level.

All the results so far have been derived under the assumption of an energy distribution from the jet axis  $\propto \theta^{-2}$  in the interval  $0 \leq \theta \leq \pi/2$ . However, close to the axis this divergence must naturally have a cutoff which we represent by a core of size  $\theta_c$ . We now explore how our results vary by allowing for the presence of a core in the inner part of the jet and an outer cutoff at some large angle  $\theta_j$ , where the luminosity drops rapidly to zero rather than following the profile in Eq. (5). In this case the peak photon luminosity is given by  $L_P(\theta)$  as in Eq. (5) for  $\theta_c < \theta < \theta_j$ , and by  $L_P(\theta = \theta_c)$  for all the angles  $\theta \leq \theta_c$ . Hence the cumulative  $\theta$  distribution is given by

$$N(< \theta) = \begin{cases} 0 & \theta < \theta_c \\ \int_0^{\theta_c} d\theta' \frac{dn[\theta', L(\theta_c)]}{d\theta'} \equiv N_c & \theta = \theta_c \\ N_c + \int_{\theta_c}^{\theta} d\theta' \frac{dn[\theta', L(\theta')]}{d\theta'} \equiv N_j & \theta_c < \theta < \theta_j \\ N_j & \theta > \theta_j \end{cases}. \quad (12)$$

For the case where the increase in luminosity saturates at an angle  $\theta_c$  from the jet axis (left panel of Fig. 2), the number of observed bursts with break angle  $\theta < \theta_c$  is smaller than the corresponding number at the same observed  $\theta$  for the distribution with  $\theta_c = 0$  (solid line in the figure). This is because  $z_{\max}$  saturates to the value given by the solution of Eqn. (2) with  $L = L_c$  for all  $\theta \leq \theta_c$ , whereas when there is no core<sup>6</sup>,  $z_{\max}$  is larger for the jet angles  $\theta < \theta_c$ . The situation is reversed in the case of a jet with  $\theta_c = 0$  but a total aperture  $\theta_j < \pi/2$  (right panel of Fig.2). The number of bursts with observed break angle  $\theta > \theta_j$  is zero. Therefore, in order for the normalization (i.e. total number of observed bursts) to be the same for any  $\theta_j$ , the cumulative number  $N(< \theta)$  for the case  $\theta_j < \pi/2$  must be larger than the corresponding number for the case  $\theta_j = \pi/2$  (solid line in the figure).

---

<sup>6</sup>Note that when we say here “no core” or  $\theta_c = 0$ , we mean an infinitesimally small core, as there would be a formal divergence in the energy if  $\theta_c$  were precisely equal to zero.



The probability remains of the same order by varying the core angle  $\theta_c$  in the range  $0 \lesssim \theta_c \lesssim 0.055$ , and drops as  $\theta_c$  is increased above 0.055 (which is the smallest angle in the data set). Similarly, no significant variation in the probability is found as the outer boundary of the jet angle,  $\theta_j$  is decreased from  $\pi/2$  to 0.55 rad, which is the largest observed break angle. In short, the current data is too poor to constrain either the size of the core,  $\theta_c$ , or the outer size of the jet,  $\theta_j$ , beyond the trivial statement that this range must include the range of observed opening angles. It should however be remarked that, whereas the current data on the observed  $\theta_{\text{break}}$  do not allow to pin down the values of the model parameters  $\theta_c$  and  $\theta_j$ , the type of analysis that we are proposing has the potentiality to further constrain details of the model once a larger sample of jet opening angles is gathered.

## 5. Conclusions

A natural framework for the interpretation of achromatic breaks in the afterglow light curves is the presence of jets in the GRB ejecta. There is however a certain degree of degeneracy in the resulting light curves between the case where the jet has uniform energy profile and a sharp edge, and where it has instead a variable energy profile. Distinguishing between the two scenarios is especially important in order to have a proper estimate of the GRB event rates, and a better understanding of the physics of the GRB explosion. A particularly useful discriminant of the two jet scenarios is the distribution of the observed break times, which can be theoretically predicted in the structured jet model, and compared to the data.

In this paper, we have derived such distribution and compared it to the observed sample of data on  $\theta_{\text{break}}$ . We found that the observed data set, although a small sample, is consistent with the predictions of the structured-jet model. We should however remark that the alternative “uniform” model, in which there is a direct correlation between the observed opening angle and the physical jet angle, cannot be ruled out by this approach. However, if, as more data becomes available, the agreement with the predictions of the structured jet model remains intact, it would be very contrived to justify it within the framework of the uniform jet. This model, in fact, does not make any prediction for the distribution of opening angles. One would then need to invoke an explanation for why there is the same number of bursts for each logarithmic interval of opening angle.

Besides performing a first attempt to test the structured-jet model, we have shown that this model offers a number of predictions which may be testable with future, larger datasets. The predicted opening angle distribution shown in Figure 1 (which assumes the BATSE detection threshold), has a distinct peak at  $\theta \sim 0.12$  rad. We predict that future, more sensitive missions will predict more bursts with large opening angles. Specifically, we estimate that the opening angle distribution for the SWIFT mission will peak near  $\theta \sim 0.3$  rad. Surprisingly, in this model the average redshift is only a weak function of the sensitivity and consequently we expect no increase in the *average* redshift detected by the next generation of gamma-ray instruments.

Another prediction that the structured-jet model makes, regards the number of GRBs in the local universe. Our “standard” SFR model yields  $R_{\text{GRB}}(z = 0) \sim 0.5 \text{ Gpc}^{-3} \text{ yr}^{-1}$ . Combining this with the local galactic density  $\approx 0.0048 \text{ Mpc}^{-3}$  (Loveday et al. 1992) one obtains  $\approx 0.1$  GEM (galactic events per Myr). This is an interesting number for detection of local GRB remnants (Loeb & Perna 1998; Efremov et al. 1998; Perna et al. 2000). For the uniform jet model, precise rates are more difficult to estimate, as they depend on the assumed luminosity function, or equivalently the intrinsic jet angle distribution which is not known apriori for this model. If one were to assume that  $dn/d\theta \propto \theta$  as in the structured jet model, this would result in a logarithmic correction factor,  $(1 + \log[(\pi/2)/\theta_c])$ , to the rate that we estimated here for the structured jet model<sup>7</sup>. The total energy output of GRBs would however remain the same, as in the structured jet model the total energy of each burst is also corrected by a logarithmic factor with respect to the total energy of each burst in the uniform case.

We thank the referee for a very careful and thoughtful review of our manuscript. RP and DAF thank the California Institute of Technology for its kind hospitality during the time that part of this work was carried out. RS holds a senior Sherman Fairchild fellowship. This research was partially supported by a NASA grant to RS. The NRAO is a facility of the National Science Foundation operated under cooperative agreement by Associated Universities, Inc.

## REFERENCES

- Bloom, J. S., Frail, D. A. & Sari, R. 2001, *AJ*, 121, 2879
- Bloom, J. S., Kulkarni, S. & Frail, D. A., 2003, submitted to *ApJ*
- Covino, S. *et al.* 1999, *A&A*, 348, L1.
- Efremov, Y. N., Elmegreen, B. G., & Hodge, P. W. 1998, *ApJ*, 501, L163
- Frail, D. et al. 2001, *ApJ*, 562, 65
- Gnedin, N. Y. & Ostriker, J. P. 1997, *ApJ*, 486, 581
- Harrison, F. A. *et al.* 1999, *ApJ*, 523, L121.
- Harrison, F. A. *et al.* 2001, *ApJ*, 559, 123.
- Lloyd-Ronning, N. M., Fryer, C. L. & Ramirez-Ruiz, E. 2001, *ApJ* in press (astro-ph/0108200)
- Loeb, A., & Perna, R. 1998, *ApJ*, 533, L35
- Loveday, J., Peterson, B. A., Efstathiou, G., Maddox, S. J. 1992, *ApJ*, 390, 338
- Madau, P., Ferguson, H. C., Dickinson, M. E., Giavalisco, M., Steidel, C. C. & Fruchter, Andrew, 1996, *MNRAS*, 283 1388

---

<sup>7</sup>The correction is expected to be less than an order of magnitude as  $\theta_c \gtrsim 1/\Gamma$ .

- Mallozzi, R. S., Pendleton, G. N., & Paciesas, W. S. 1996, *ApJ*, 471, 636
- Nicastro, L. et al. 1999, *A&AS*, 138, 437
- Norris, J. P., Marani, G. F. & Bonnell, J. T. 2000, *ApJ*, 534, 284
- Panaitescu, A. P. & Kumar, P. 2002, 571, 779
- Perna, R., Raymond, J., & Loeb, A. 2000, *ApJ*, 533, 658
- Postnov, K. A., Prokhorov, M. E., Lipunov, V. M. 2001, *Astronomy Report*, 45, 236
- Rhoads, J. E. 1997, *ApJ*, 487, L1
- Rhoads, J. E. 1999, *A&AS*, 138, 539
- Rowan-Robinson, M. 1999, *Ap&SS*, 266, 291
- Sari, R., Piran, T. & Halpern, J. 1999, *ApJ*, 519, L17
- Salmonson, J. D., 2000, *ApJL*, 544, 115
- Rossi, E., Lazzati, D. & Rees, M. J. 2002a, *MNRAS*, 332, 945
- Rossi, E., Lazzati, D., Salmonson, D. J. & Ghisellini, G. 2002b, *Proceeding of the workshop "Beaming and Jets in Gamma Ray Bursts"*, Copenhagen, August 12-30, 2002
- Stanek, K. Z., Garnavich, P. M., Kaluzny, J., Pych, W., & Thompson, I. 1999, *ApJ*, 522, L39
- Vrba, F. et al. 2000, *ApJ*, 528, 254
- Wang, W., Woosley, S. E. & MacFadyen, A. J., submitted to *ApJ*, (astro-ph/0207436)
- Wijers, R. A. M. J. *et al.* 1999, *ApJ*, 523, L33.
- Zhang, B. & Meszaros, P. 2002, *ApJ*, 571, 876

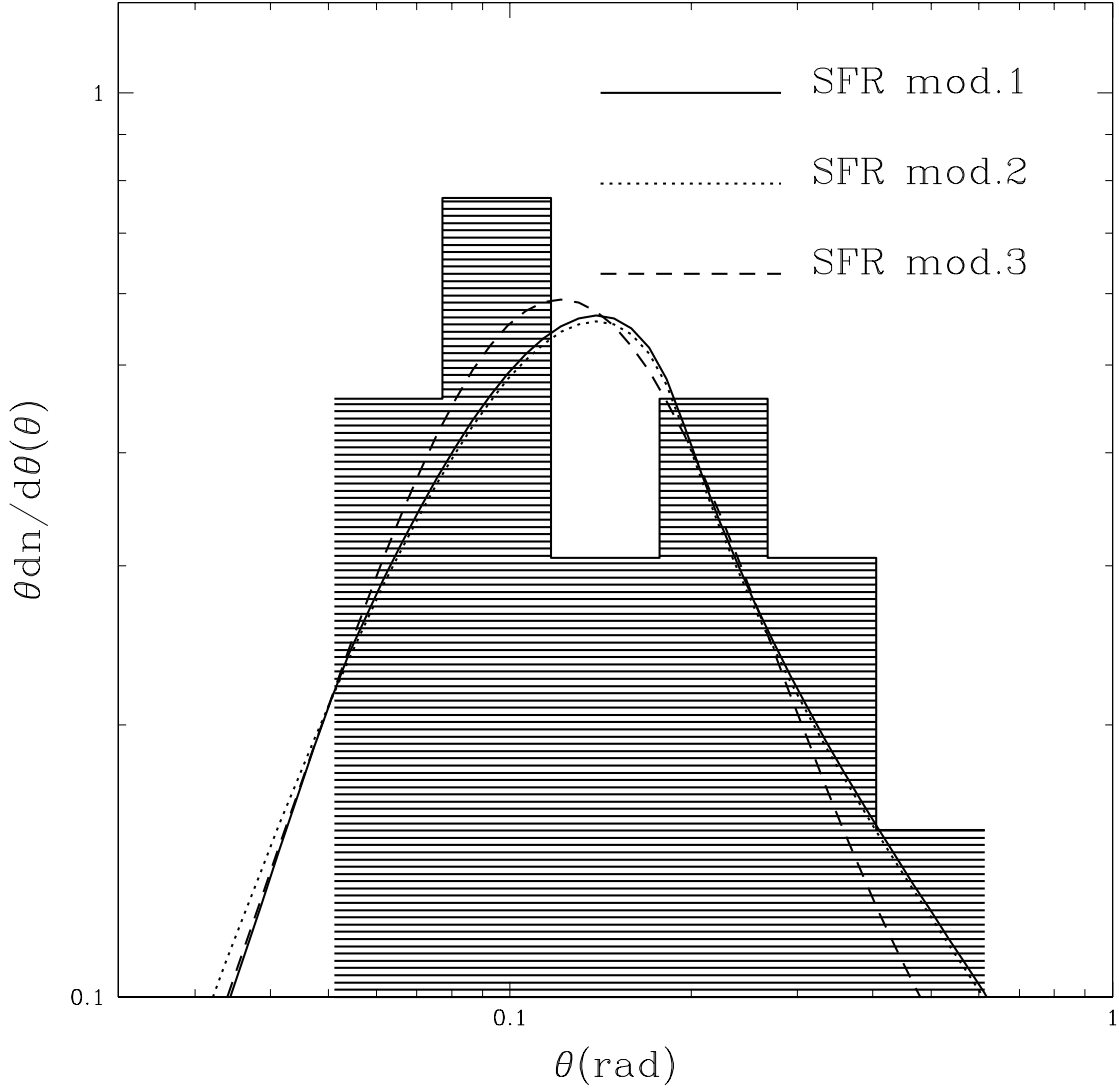


Fig. 1.— Distribution of observed jet angles for different star formation rates: in model 1 the Rowan-Robinson SFR is assumed up to  $z \geq 10$ , and a rapid drop is assumed at larger redshifts as in the numerical simulations of Gnedin & Ostriker. In model 2, no dropout is assumed for  $z \gtrsim 10$ , while model 3 uses the Madau SFR. The histogram shows the observed distribution from the data available so far for a sample of 16 bursts.

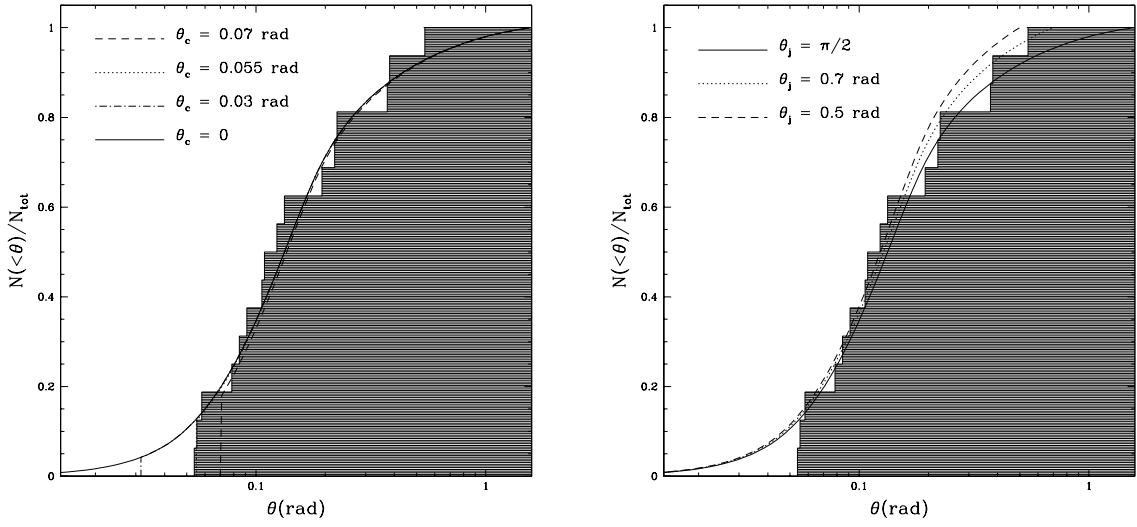


Fig. 2.— Left panel: Cumulative distribution for the SFR model 1, and various values of the jet core. Here  $\theta_j = \pi/2$ . Right panel: Cumulative distribution for the SFR model 1, and various values of the jet aperture. Here  $\theta_c = 0$ .

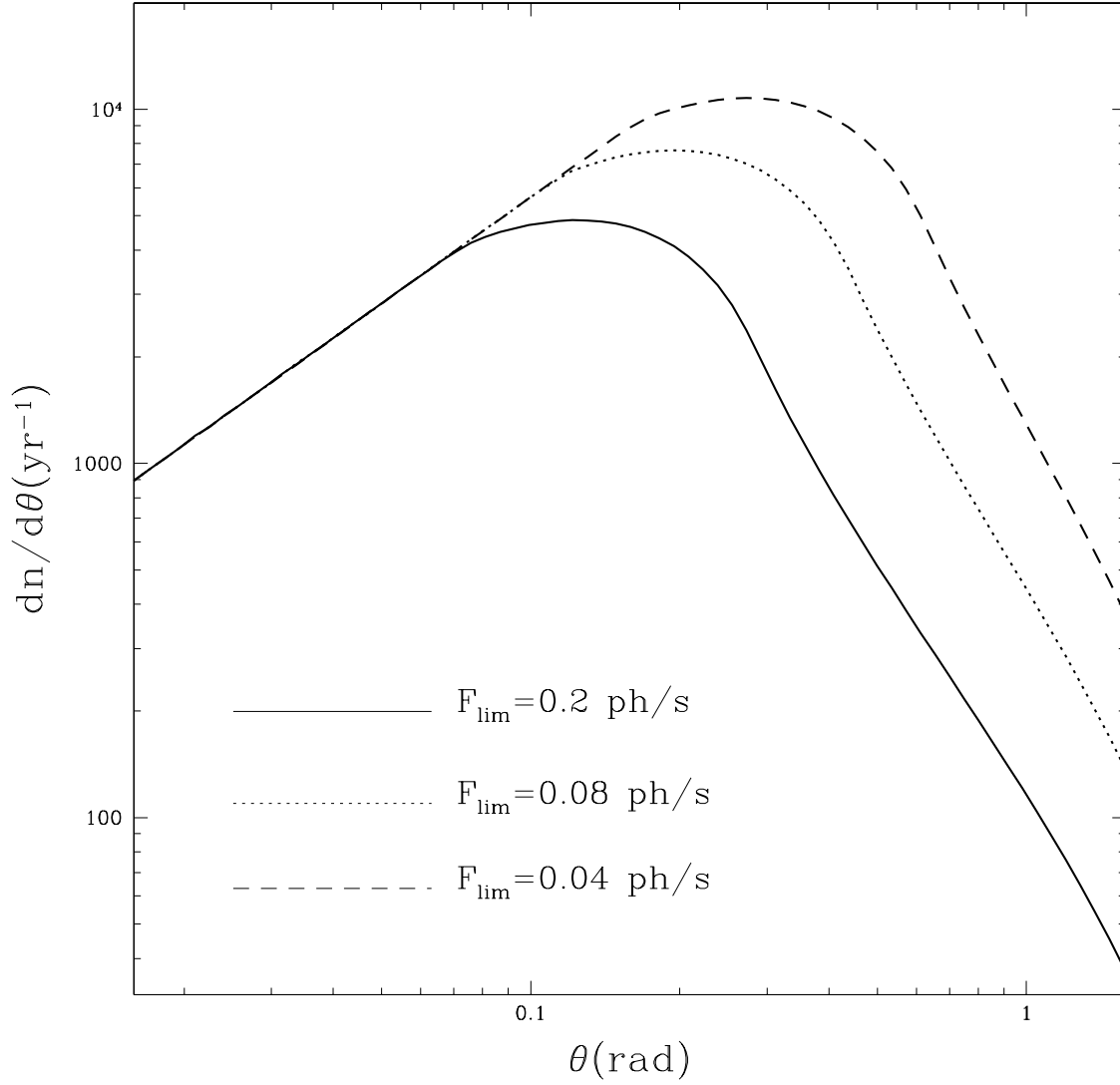


Fig. 3.— Probability distribution for the observed jet angle  $\theta$  for different values of the survey sensitivity threshold. The higher the sensitivity of the survey, the larger is the mean beaming angle  $\theta$  that is observed. Here  $\theta_j = \pi/2$  and  $\theta_c = 0$  for the SFR model 1.